



HAL
open science

The Precipitation Inferred from Soil Moisture (PrISM) near real-time rainfall product: evaluation and comparison.

Thierry Pellarin, Carlos Román-Cascón, Christian Baron, Rajat Bindlish,
Luca Brocca, Pierre Camberlin, Diego Fernández-Prieto, Yann H. Kerr,
Christian Massari, Gérémy Panthou, et al.

► **To cite this version:**

Thierry Pellarin, Carlos Román-Cascón, Christian Baron, Rajat Bindlish, Luca Brocca, et al.. The Precipitation Inferred from Soil Moisture (PrISM) near real-time rainfall product: evaluation and comparison.. Remote Sensing, 2020, 12 (3), pp.481. 10.3390/rs12030481 . hal-02531523

HAL Id: hal-02531523

<https://hal.science/hal-02531523>

Submitted on 31 Dec 2020

HAL is a multi-disciplinary open access archive for the deposit and dissemination of scientific research documents, whether they are published or not. The documents may come from teaching and research institutions in France or abroad, or from public or private research centers.

L'archive ouverte pluridisciplinaire **HAL**, est destinée au dépôt et à la diffusion de documents scientifiques de niveau recherche, publiés ou non, émanant des établissements d'enseignement et de recherche français ou étrangers, des laboratoires publics ou privés.

1 Type of the Paper (Article, Review, Communication, etc.)

2 The Precipitation Inferred from Soil Moisture 3 (PrISM) near real-time rainfall product: evaluation 4 and comparison

5 Thierry Pellarin ^{1,*}, Carlos Román-Cascón ^{1,2}, Christian Baron ³, R. Bindlish ³, Luca Brocca ⁵, Pierre
6 Camberlin ⁶, Diego Fernández Prieto ⁷, Yann H. Kerr ⁸, Christian Massari ⁵, G. Panthou ¹, B.
7 Perrimond ¹, N. Philippon ¹, and G. Quantin ¹

8 ¹ Univ. Grenoble Alpes, CNRS, IRD, Grenoble INP, IGE, Grenoble F-38000, France; thierry.pellarin@univ-
9 grenoble-alpes.fr

10 ² Laboratoire d'Aérodynamique, Université Toulouse Paul Sabatier, CNRS, France;

11 ³ CIRAD-ES, TA C-91/MTD, 500 rue Jean François Breton, 34093 Montpellier Cedex 5, France ;

12 ⁴ NASA Goddard Space Flight Center, Greenbelt, MD

13 ⁵ Research Institute for Geo-Hydrological Protection, Via Madonna Alta 126, Perugia, Italy;

14 ⁶ Centre de Recherches de Climatologie / Biogéosciences, UMR 6282 CNRS, Université Bourgogne Franche-
15 Comté, 21000 Dijon, France ;

16 ⁷ EO Science, Applications and Climate Department, Largo Galileo Galilei, 1, 00044 Frascati, Italy;

17 ⁸ CESBIO (CNRS/UPS/IRD/CNES), 18 av. Edouard Belin, bpi 2801, 31401 Toulouse cedex 9, France;

18

19 * Correspondence: thierry.pellarin@univ-grenoble-alpes.fr

20 Received: date; Accepted: date; Published: date

21 **Abstract:** Near real time precipitation is essential to many applications. In Africa, the lack of dense
22 raingauge networks and ground weather radars makes the use of satellite precipitation products
23 unavoidable. Despite major progresses in estimating precipitation rate from remote sensing
24 measurements over the past decades, satellite precipitation products still suffer from quantitative
25 uncertainties and biases compared to ground data. Consequently, almost all precipitation products
26 are provided in two modes: a real-time mode (also called early-run or raw product) and a corrected
27 mode (also called final-run, adjusted or post-processed product) in which ground precipitation
28 measurements are integrated in algorithms to correct for bias generally at a monthly timescale. This
29 paper describes a new methodology to provide a near-real-time precipitation product based on
30 satellite precipitation and soil moisture measurements. Recent studies have shown that soil
31 moisture intrinsically contains information on past precipitation and can be used to correct
32 precipitation uncertainties. The PrISM (Precipitation inferred from Soil Moisture) methodology is
33 presented and its performance is assessed for five in situ rainfall measurement networks located in
34 Africa in semi-arid to wet areas: Niger, Benin, Burkina Faso, Central Africa, and East Africa. Results
35 show that the use of SMOS soil moisture measurements in the PrISM algorithm most often improves
36 the real-time satellite precipitation products, and provides results comparable to existing adjusted
37 products such as TRMM-3B42, GPCP and IMERG which are available a few weeks or months after
38 their detection.

39 **Keywords:** Precipitation; Soil moisture; Africa; satellite rainfall products; comparison

40

41 1. Introduction

42

43 Rainfall is a crucial resource in Africa, where large parts of the population rely on rainfed
44 agriculture. The continent is also known for its vulnerability to rainfall variability that impacts the
45 natural resources (water, vegetation) and subsequently the wellness of populations, in societies

46 where economy is based mainly on agriculture [1]. Knowledge on rainfall spatio-temporal
47 distribution is essential to various applications such as water-resource and land-use management,
48 agricultural crop yield estimates, flood nowcasting, dam management, ground-water recharge
49 estimates and irrigation demand. Rain-gauges provide the most common and most direct
50 measurement of point precipitation at the surface, therefore they are generally assumed as the most
51 accurate method to measure precipitation. Unfortunately, Africa is a region where the ground-based
52 rain-gauge network is of very low density and operational radar installations are almost non-existent
53 [2]. Furthermore, the gauge networks have been degrading over the last few decades [3].
54

55 In this context, satellite-based precipitation products represent an unavoidable alternative for
56 providing precipitation knowledge in Africa. In recent decades, significant progress has been made
57 in satellite precipitation estimation. This progress is mostly due to the introduction of new sensors
58 (e.g. Global Precipitation Measurement Core Observatory satellite), but also to the improved sensor
59 accuracy, and efficiency of proposed algorithms that take advantage of the many observational data
60 (including multi-channel VIS/IR sensors, and passive microwave). Many studies have been dedicated
61 to the evaluation of these different satellite precipitation products in Africa [4-8]. Without being
62 exhaustive, the main conclusions of these studies can be summarized as follows: (i) the state-of-the-
63 art products perform relatively well at monthly and decadal time steps [4, 9, 10] with a decreasing
64 performances for finer timescales; (ii) most products satisfactorily reproduce the main features of the
65 rainfall regime [4, 5]; (iii) real-time products exhibit moderate to high (positive or negative) biases [4]
66 whereas adjusted or post-processed products, in which ground precipitation measurements are
67 included in algorithms to correct bias, show lower biases, (iv) there is a clear need to improve the
68 accuracy of satellite products in the estimation of accumulated rainfall [6, 11].
69

70 One potential strategy for improving satellite precipitation products is to use soil moisture
71 measurements from satellite microwave sensors. Soil moisture can be seen as the trace of
72 precipitation, and a knowledge of the temporal and spatial variability of soil moisture could benefit
73 to rainfall retrievals from space. Pioneer studies [12-17] exploited this signal to correct existing
74 satellite precipitation products. Later, [18, 19] developed the SM2RAIN approach to directly derive a
75 rainfall amount from soil moisture variations exclusively. Since 2015, these approaches were
76 improved and applied at the global scale [20, 21] and on different locations in the US [22], in Australia
77 [23], over selected sites [24] and in China [25]. One of the main advantages of these methodologies
78 based on soil moisture measurement is that they can replace, in near-real-time, scaling procedures of
79 state-of-the-art satellite precipitation and avoid significant latency for dataset availability.
80

81 This paper aims to present the latest developments in the PrISM (Precipitation Inferred from Soil
82 Moisture) algorithm originally developed by [17, 24]. The concept of PrISM is to use an existing real-
83 time precipitation product and to correct it using a soil moisture information. In addition to PrISM
84 algorithm, this paper presents an accurate evaluation of its performances for Africa, including a
85 comparison with the performance of ten additional precipitation products at the daily time-scale. In
86 order to improve the evaluation of the product in a region with very low rain-gauge coverage,
87 exclusively local, national and pan-national in situ rain gauge measurements were used to assess
88 PrISM performances and to compare with state-of-the art precipitation products. This was done to
89 avoid traditionally used products that can be tricky at fine time scales, such as the Global
90 Precipitation Climatology Center (GPCC [26]), the Global Precipitation Climatology Project (GPCP
91 [27, 28]) or the Climatic Research Unit (CRU [29]). The paper is organized as follows: section 2
92 describes the satellite and ground-based rainfall datasets, and the PrISM algorithm; section 3 presents
93 the results and a comparison with existing rainfall products; and section 4 draws conclusions and
94 perspectives.
95

96 2. Materials and Methods

97 2.1 Ground-based precipitation measurements

98

99

100 Five reference data sets based on in situ rainfall measurements are used in this study (Table 1).
 101 The first two datasets are provided by the AMMA-CATCH Observatory in Niger and Benin [30, 31].
 102 Both sites cover about $1 \times 1^\circ$ and are composed of 34 gauge stations in Niger and 30 gauge stations in
 103 Benin. A spatial interpolation (block kriging) was performed at the $0.25 \times 0.25^\circ$ spatial resolution in
 104 order to obtain a reference rainfall amount at the commonly used satellite spatial scale (0.25°). The
 105 selected 0.25° sites in Niger and Benin are respectively centered at 2.625°E ; 13.625°N and 1.625°E ;
 106 9.625°N (see Figure 1). The number of gauge stations that directly affect the rainfall amount at the
 107 0.25° resolution are 12 in Niger and 10 in Benin. The third data set is composed of 20 in situ gauge
 108 stations covering the whole of Burkina Faso. The dataset was provided by National Meteorological
 109 Department of Burkina Faso. The fourth dataset is the “WaTFor” data set which documents Western
 110 Central Africa. Built-up by [5] it contains monthly and daily in situ rainfall data collected from global
 111 datasets, national meteorological services and monitoring projects for Cameroon, Gabon, Congo and
 112 Central African Republic. Finally, the last data set is a gauge network composed of 78 stations
 113 covering 7 countries in East Africa (Ethiopia, Djibouti, Somalia, Kenya, Uganda, Tanzania and
 114 Rwanda [32]). The datasets at national scale comprise both synoptic stations (whose data are
 115 generally incorporated in post-processed products) and independent stations.

115

116

117

Table 1. Observed rainfall data sets used for evaluation.

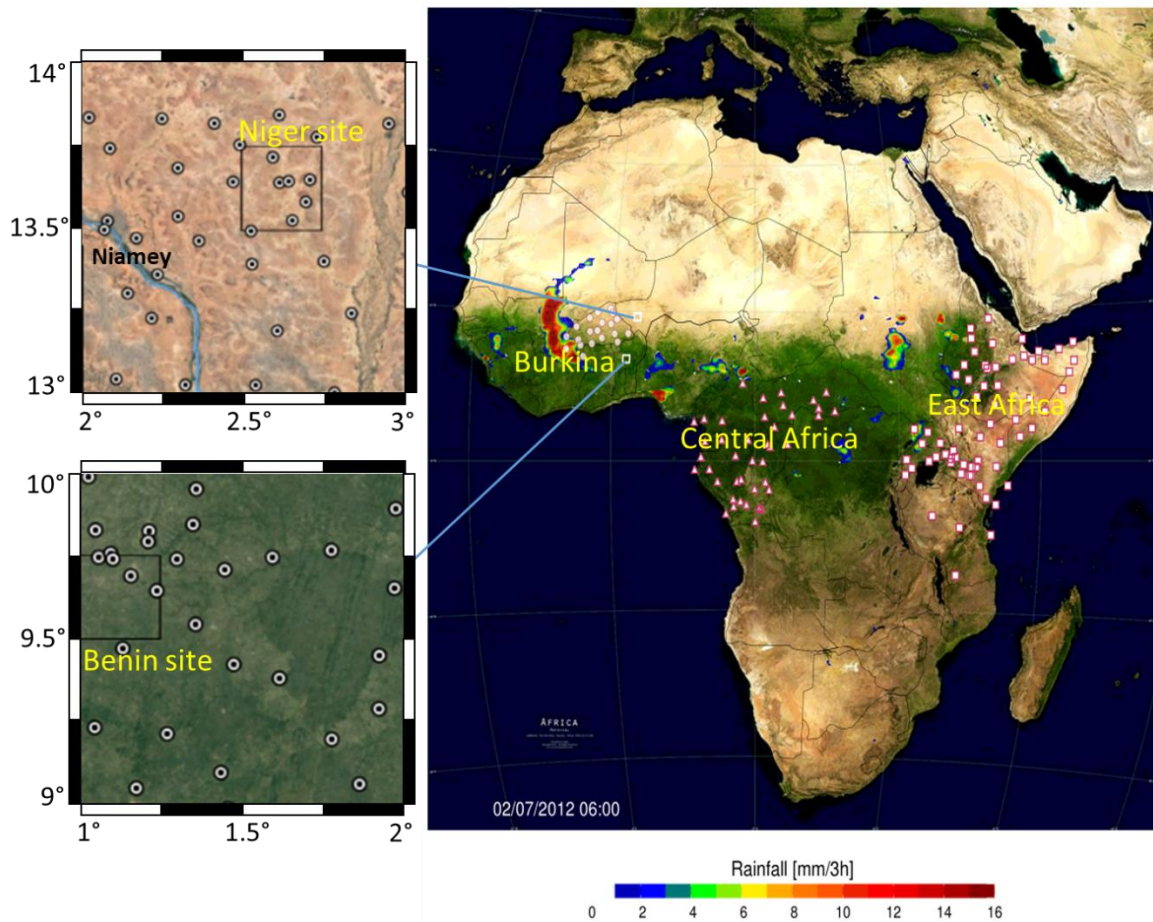
Data set	Nb stations	Period	Time scale
Niger	12	2010-2016	3h
Benin	10	2010-2016	3h
Burkina Faso	20	2010-2015	Daily
Central Africa	42	2010-2016	Daily
East Africa	78	2010-2013	Daily

118

119

120

121



122
 123 **Figure 1:** Location of the five reference ground-based rainfall data sets: Burkina Faso (20 stations), Central Africa
 124 (42 stations), East Africa (78 stations) and the two AMMA-CATCH sites located in Niger (region of Niamey) and
 125 Benin (region of Nalohou). The two squares inside the two left graphs represent the two selected 0.25° pixels in
 126 Niger and Benin. Precipitation product on top of land cover on the right map illustrates a time step (3h) of the
 127 PrISM precipitation product (2012 July 2nd 3 to 6 am).

128 2.2 Satellite precipitation products

129
 130 In addition to the PrISM product, ten existing satellite and ground-based rainfall products have
 131 been selected for the inter-comparison (Table 2). All products are provided at the 3-hour and 0.25
 132 degree resolution except TAMSAT (daily, 0.0375°), IMERG (half-hourly, 0.1°), SM2RAIN (daily,
 133 0.25°), CHIRPS (daily, 0.25°) and GPCC (daily, 1°). In order to enable an inter-comparison of the
 134 products, all the products were regrided to 0.25° spatial resolution and daily temporal resolution.
 135 Five rainfall products (out of 10) are available in real-time and are not merged with any raingauge
 136 observations. The other five products are available after a latency ranging from 7 days to 2 months
 137

138 CMORPH [33] is a rainfall estimate product based on geostationary infrared images and passive
 139 microwave data from low earth orbiting satellites. Motion vectors are determined from half-hourly
 140 geostationary infrared measurements, and used to propagate the estimates obtained from the
 141 microwave data. The CMORPH rainfall product is proposed in two modes: the CMORPH-Raw
 142 product which is not merged with any raingauge observations and the CMORPH-Adj product which
 143 use a monthly ground calibration procedure to remove bias and uncertainties. In this study, the 0.25°
 144 3-hour version of the product was used.
 145

146 TRMM 3B42 products [34] originality lies in incorporating precipitation radar and microwave
147 measurements to better evaluate rainfall intensity. It combines these data with polar-orbiting and
148 geostationary satellite images to obtain 3-hourly rainfall estimates at 0.25° spatial resolution. Similar
149 to CMORPH, the TRMM 3B42 products are available in two modes: the TRMM-3B42RT product
150 (hereafter called TRMM-Raw) available in near real-time (latency of about 7 hours) which is not
151 merged with any raingauge observations and the TRMM-3B42 product (hereafter called TRMM-Adj)
152 which includes GPCP monthly gauge aggregations and is available with a latency up to 6-week. The
153 TRMM-3B42 v7 used in this study improves upon the previous ones by incorporating additional
154 microwave and infrared data, revising the relationship between radar reflectivity and rainfall rates,
155 and using better reference data bases for bias correction.

156

157 The IMERG product, firstly released in early 2015 [35], is provided at 0.1°×0.1° spatial and half-
158 hourly temporal resolutions in three modes, based on latency and accuracy: “early” (latency of 4–6 h
159 after observation), “late” (12–18 h), and “final” (~3 months). The main difference between the early
160 and final runs is – beyond the way the different sensor measurements are propagated in time – that
161 the early run has a climatological rain gauge adjustment while the final run uses a month-to-month
162 adjustment based on GPCC gauge data. In this study, we used the IMERG-Early and IMERG-Final
163 products. The two products were upscaled to 0.25° by using a box-shaped kernel with antialiasing,
164 which approach was found to outperform simple spatial averaging and half-hourly rainfall were
165 accumulated to obtain a daily product [36].

166

167 TAMSAT (Tropical Applications of Meteorology using SATellite and ground based
168 observations) was developed at the University of Reading specifically for Africa with a spatial
169 resolution of 0.0375°. The TAMSAT method [37–39] is based on high resolution (0.0375°) METEOSAT
170 thermal-infrared observations for all of Africa, available from 1983 to the present and updated in
171 near-real time (up to 7 days). Contrary to other merged products, TAMSAT does not use Global
172 Telecommunication System (GTS) data but historical data from about 4000 stations acquired by
173 various African agencies since the early 1990s [40]. We used the TAMSAT V3.0 version product [38]
174 available at the daily time scale. Similar to IMERG, the product was regridded to the 0.25° spatial
175 resolution, and is called TAMSAT_025.

176

177 The GPCC daily product is provided by the Global Precipitation Climatology Center [26], and
178 is available since 1 January 2009 with a spatial sampling grid of 1°. GPCC is a gridded gauge-analysis
179 product derived from quality-controlled station data (more than 85,000 different stations). This
180 dataset is characterized by an uneven spatial distribution: some regions are characterized by dense
181 rain gauge networks (Europe, US, China) while other regions such as Africa, Amazonia and Northern
182 areas suffer from low density networks. To enable comparison with other products, GPCC was
183 downscaled to 0.25° spatial resolution with a linear interpolation method.

184

185 CHIRPS (Climate Hazards group Infrared Precipitation with Stations) dataset is a quasi-global
186 (50°S–50°N), high resolution (0.05°), daily, pentadal, and monthly precipitation dataset [41]. CHIRPS
187 uses the Tropical Rainfall Measuring Mission Multi-satellite Precipitation Analysis version 7 (TMPA
188 3B42 v7) to calibrate global Cold Cloud Duration (CCD) rainfall estimates. CHIRPS incorporates
189 station data in a two phase process. In the first phase, Meteorological Organization’s Global
190 Telecommunication System (GTS) gauge data are incorporated and a 2-day latency product is
191 available. In the second phase, station data are combined with monthly (and pentadal) high
192 resolution rainfall estimates to produce a second product with a latency of about 3 weeks. The version
193 used in this study is the second product available at the daily and 0.25 degree resolution.

194

195 Similar to PrISM, SM2RAIN precipitation product [18, 19] takes advantage of satellite soil
196 moisture observations to derive a precipitation product. SM2RAIN is based on the inversion of the
197 soil water balance equation and allows to estimate the amount of water entering the soil by using as

198 input soil moisture observations from in situ or satellite sensors (e.g., [20, 42-44]. The SM2RAIN
 199 product used in this study is the GPM+SM2RAIN precipitation dataset (hereafter called SM2RAIN)
 200 which is based on the integration of IMERG-ER with SM2RAIN-based rainfall estimates derived from
 201 ASCAT, SMOS and SMAP L3 soil moisture products. The merging methodology is using an Optimal
 202 Linear Combination approach, OLI [46, 47]. This approach provides an analytically optimal linear
 203 combination of ensemble members (precipitation products in this case) that minimizes mean square
 204 error when compared to a reference dataset. The dataset is currently available for Africa and South
 205 America (2015-2018), Europe, India, Contiguous United States and Australia (2015-2017) and can be
 206 downloaded at <https://doi.org/10.5281/zenodo.3345323>.

208 Table 2. Inventory of all satellite rainfall products data sets used in the study. To enable fair comparison of all
 209 products, each product was regridded to the 0.25° spatial resolution and daily time-scale.

Data set	Spatial Resolution	Time-scale	Period	Latency	Ground calibration
PrISM	0.25°	3-hourly	2010-present	~5 day	no
CMORPH-Raw	0.25°	3-hourly	1998-present	18 h	no
TRMM-RT	0.25°	3-hourly	1998-present	~6 h	no
IMERG-Early	0.1°	30 min	03/2015-present	~12 h	no
TAMSAT-v3.0	0.0375°	Daily	1983-present	~2 days	no
SM2RAIN	0.25°	Daily	2015-2018	~5 days	no
CHIRPS-v2.0	0.25°	Daily	1981-present	~3 weeks	yes
GPCC	1°	Daily	2009-present	15-45 days	yes
CMORPH-Adj	0.25°	3-hourly	1998-present	>1 month	yes
TRMM-3B42	0.25°	3-hourly	1998-present	>1 month	yes
IMERG-Final	0.1°	30 min	03/2015-present	>1 month	yes

210

211 2.3 The SMOS soil moisture dataset

212 The Soil Moisture and Ocean Salinity [48, 49] satellite was launched in November 2009 and
 213 started delivering data on January 2010. The primary goals of this Earth Explorer mission are to
 214 measure globally and frequently surface soil moisture over land and sea surface salinity over the
 215 oceans. The SMOS data used in the study as the main input to the PrISM algorithm corresponds to
 216 the CATDS level-3 soil moisture data obtained through <https://www.catds.fr> site. The SMOS-L3SM
 217 products are in NetCDF format and were regridded from the EASE 25km grid to the 0.25°x0.25°
 218 regular grid retained in the present study using the closest neighbor.

219 2.4 The PrISM methodology

220

221 The concept of the PrISM (Precipitation Inferred from Soil Moisture) methodology is to exploit
 222 remote sensing soil moisture measurements to correct the amount of rainfall estimated by an existing
 223 satellite rainfall product (CMORPH-Raw in this study). It makes use of a simple soil moisture /
 224 precipitation model and an assimilation scheme.

225

226 2.4.1 The API soil moisture / precipitation model

227

228 The API (Antecedent Precipitation Index) model is a simple model designed to simulate a soil
 229 moisture dynamic based on precipitation data. The API model is defined as:

230

$$API_{(t)} = API_{(t-1)} \cdot e^{-\frac{\Delta t}{\tau}} + P_{(t)} \quad (\text{Eq.1})$$

231

232

233

234

235

236

237

238

239

240

241

242

243

244

245

246

247

248

249

250

251

252

253

254

255

256

257

258

259

260

261

262

263

264

265

266

267

268

269

270

271

272

273

274

275

276

277

278

279

where $P(t)$ is the rainfall accumulation (in mm) during the period Δt (in h) and τ a parameter that describes the drying-out soil moisture velocity (in h). The API index is a simple proxy of the soil moisture dynamic (in mm). Recently, [50] proposed a slight modification of the original API model in order to improve its accuracy and enable the calculation of volumetric soil moisture in m^3/m^3 instead of an index expressed in mm. The new version of the API model contains two modifications: (i) it accounts for the degree of saturation of the soil before a rain event; and (ii) the soil moisture is now limited by the saturation value. These modifications of the relationship add three parameters: d_{soil} an equivalent soil thickness (in mm), θ_{sat} the soil moisture value at saturation (in m^3/m^3) and θ_{res} the residual soil moisture (in m^3/m^3). The new version of the API model (hereafter referred as the API model) is written:

$$\theta_{(t)} = (\theta_{(t-1)} - \theta_{\text{res}}) \cdot e^{-\frac{\Delta t}{\tau}} + (\theta_{\text{sat}} - (\theta_{(t-1)} - \theta_{\text{res}})) \cdot \left(1 - e^{-\frac{P(t)}{d_{\text{soil}}}}\right) + \theta_{\text{res}} \quad (\text{Eq.2})$$

245

246

247

248

249

250

251

252

253

254

255

256

257

258

259

260

261

262

263

264

265

266

267

268

269

270

271

272

273

274

275

276

277

278

279

where $\theta(t)$ is the surface soil moisture in m^3/m^3 , τ is the soil moisture drying-out velocity (in h), and $P(t)$ is the cumulative precipitation in mm during the Δt period (in h). It requires the use of a precipitation product at infra-daily resolution (3 hours or less) to determine when rainfall occurs compared to SMOS ascending (6am) or descending (6pm) orbits. A sensitivity study was conducted over 10 sites at the global scale [24] to derive the best 4 parameters of the API model. Authors showed that a constant value for $\theta_{\text{sat}} = 0.45 \text{ m}^3/\text{m}^3$ provided reliable results. On the contrary, a spatial distribution of the θ_{res} and d_{soil} parameters is required and as well as a spatiotemporal distribution of the τ parameter.

The residual soil moisture is the minimal value of soil moisture on a given pixel. Based on surface soil moisture measurements obtained over the 10 sites presented in [24], the simple following formulation was proposed:

$$\theta_{\text{res}} = 0.04676 + 0.05936 (\overline{NDVI}) - 0.00136 (\overline{Tair}) \quad (\text{Eq.3})$$

259

260

261

262

263

264

265

266

267

268

269

270

271

272

273

274

275

276

277

278

279

with \overline{Tair} (in °C) is the annual mean 2m air temperature (source MERRA, 2013) and \overline{NDVI} is the annual mean NDVI value provided by ESA-CCI-LC-L4-NDVI (Spot VGT, 2015). Globally, residual soil moisture values range from 0.017 to 0.099 m^3/m^3 at the global scale and from 0.017 to 0.060 m^3/m^3 in Africa.

The d_{soil} coefficient (in mm) describes the rapidity of soil moisture wetting during a rainfall event and is related to the soil thickness. The thinner (thicker) the soil layer, the faster (slower) the soil wetting. Over 9 out of the 10 sites studied in [24], it was found that a d_{soil} value of 35 mm was adequate compared to in situ soil moisture dynamic. This is consistent with soil moisture depth sensors located at 5 cm depth. However, on the Niger site, a value of d_{soil} equal to 100 mm was required to reproduce observed in situ soil moisture dynamics. It was concluded that this parameter can be related to the presence/absence of vegetation. In regions without vegetation, soils are often degraded with an impermeable crust associated with a low infiltration rate. A simple sigmoid relationship based on mean annual NDVI (ESA-CCI-LC-L4-NDVI, 2015) was proposed in this study as :

$$d_{\text{soil}} = 120 - \frac{80}{1 + 178482301 e^{(-100 * \overline{NDVI})}} \quad (\text{Eq.4})$$

276

277

278

279

Globally, d_{soil} values range from 40 mm (almost everywhere) to 120 mm in arid and semi-arid areas.

280 The τ parameter in Eq.2 describes the drying-out velocity of the surface soil moisture due to both
 281 evapotranspiration and infiltration rate. Consequently, this parameter should depends on both soil
 282 hydraulic properties and atmospheric forcing (air temperature, wind velocity, solar radiation). In a
 283 first approximation, it was shown in this study that τ value can be appropriately estimated with 30-
 284 days smoothed air temperature (T_{air}) using the following relationship:

$$285 \tau(t) = 400 - \left(\frac{350}{1 + e^{-0.1(T_{air} - 7.5)}} \right) \quad (\text{Eq.5})$$

287 where 30-days smoothed T_{air} values ($^{\circ}\text{C}$) are obtained from MERRA-2 database (3-hours, 2013). At
 288 the continental scale of Africa, the τ parameter ranges from 80 h to 350 h.

291 2.4.2 The CDF matching procedure

292 The PrISM methodology is based on the assimilation of the SMOS soil moisture retrievals into the
 293 API model (Eq.2). Thus, a preliminary work consists in scaling the SMOS soil moisture retrievals to
 294 the API simulation using a simple CDF-matching procedure. To that end, a reference rainfall dataset
 295 was selected to provide a reference soil moisture simulation with the API model at the Africa scale.
 296 The evaluation of two adjusted products (CMORPH-adj and TRMM-3B42) against in situ rainfall
 297 measurements in Niger and Benin sites led to the selection of the CMORPH-Adj precipitation product
 298 as the reference for the CDF-Matching procedure. Then, the API model (Eq. 2) was run for the whole
 299 of Africa using CMORPH-Adj precipitation product and parameters were derived from Eq. 3, 4 and
 300 5. Based on the obtained reference soil moisture simulation (2012), a calculation of the two linear
 301 CDF-matching coefficients ($p1$ and $p2$) was made to scale the SMOS L3SM to the reference soil
 302 moisture. The scaled SMOS values ($SMOS_{CDF}$) are assumed to be linearly related to SMOS original
 303 values as:

$$304 SMOS_{CDF} = p1 + p2 \cdot (SMOS) \quad (\text{Eq.6})$$

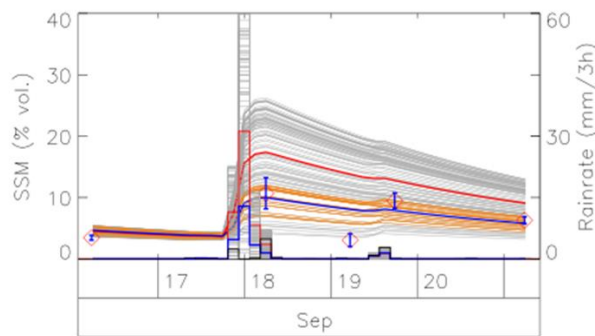
$$305 \text{with } p2 = \frac{\sigma_{SMmodel}}{\sigma_{SMsmos}} \quad \text{and} \quad p1 = \overline{SM_{model}} - p2 \cdot (\overline{SM_{smos}})$$

311 2.4.3 The Particle Filter assimilation scheme

312 Among the various existing assimilation schemes, the Particle Filter (PF) is an original method
 313 based on random stochastic perturbations of the precipitation forcing that explicitly simulates the
 314 consequences of precipitation uncertainties in the associated soil moisture outputs [51-53]. It is
 315 suitable for non-linear models and makes no assumption on the prior and posterior distributions of
 316 the model states. This property of the PF makes it more suitable for this study compared to ensemble
 317 based data assimilation approaches whose optimality and performance depend on the linearity
 318 between input and output variables, having Gaussian distributed errors, as for example in the
 319 Ensemble Kalman Filter [54, 55]. For a mathematical or formal description of PF, the reader should
 320 referred to [56].

321 The concept is a pixel-based approach. An illustration of the PF assimilation method is shown
 322 in Figure 2 (Niger site, 2015). Once there is a new SMOS soil moisture retrieval on a given pixel, an
 323 assimilation window which contains the five last SMOS retrievals is defined. The length, i.e. the
 324 number of SMOS retrieval within each assimilated sub-period was chosen after a sensitivity study
 325 (not shown) and represents a compromise between too short periods (giving much weight to
 326 individual SMOS uncertainties) and too long periods which reduce the operational interest of the
 327 methodology. Thus, the API model is forced with the real-time satellite rainfall product (CMORPH-
 328 Raw in this study) that we aim to correct and which is represented as red "bars" in Figure 2. The red
 329 curve in Figure 2 represents the soil moisture simulated by the model forced with this real-time
 330
 331

332 satellite rainfall. Then, the real-time satellite rainfall is used to generate 100 random rainfall time
 333 series (number tested in sensitivity experiments) using random stochastic perturbations (grey “bars”
 334 in Figure 2). These new rainfall time series are used to force the API model (Eq.2) to obtain an
 335 ensemble of soil moisture predictions (i.e., 100 soil moisture time series associated to 100 different
 336 rainfall time series, grey curves in Figure 2). The random stochastic perturbations of rainfall is done
 337 using the following simple multiplicative relationship: $Rain(t,i) = Rain(t) \cdot a(i)$ with $a(i)$ a random
 338 number between 0 and 2 for $i=1,100$ (uniform distribution). Figure 2 clearly shows that the random
 339 rainfall can’t exceed twice the amount of the initial rainfall. Then, the SMOS retrievals are used to
 340 select the 30 most probable soil moisture trajectories which minimize the RMSE. Finally, the corrected
 341 rainfall amount corresponds to the average of the 30 most probable rainfall time-series. The corrected
 342 rainfall estimate is associated with an uncertainty calculated as the difference between the maximum
 343 and the minimum value of the 30 most probable rainfall time-series.
 344



345
 346

347 **Figure 2:** Illustration of the PF assimilation scheme for the Niger site. The initial satellite precipitation rate (in
 348 red) produces the associated soil moisture evolution (in red). Stochastic perturbations of the initial satellite
 349 precipitation rate produce an ensemble of potential soil moisture evolutions (in grey). The SMOS retrievals (5
 350 orange diamonds) are used to select the most probable soil moisture curves (in orange) and to calculate the
 351 averaged soil moisture (in blue), which is associated with a specific precipitation rate (in blue). In this case, a
 352 decrease of the initial satellite precipitation rate is proposed which is consistent with in situ precipitation
 353 measurements (in black).

354 The process is repeated when a new SMOS measurement is available. Consequently, each
 355 rainfall event is considered 4 times (a period of 5 successive SMOS measurements provides 4
 356 intervals) and the final rainfall rate correction is the averaged value of the 4 proposed corrected
 357 rainfall rates.
 358

359 As the method is based on a modification of the precipitation rate of an existing product, it is
 360 not possible to create any rain event. It is also difficult to completely remove an existing rain event
 361 even if it is possible to significantly reduce it. Therefore, the method has a low impact on scores
 362 usually used in satellite precipitation product comparisons such as probability of detection (POD)
 363 and false-alarm ratio (FAR).

364 3. Results

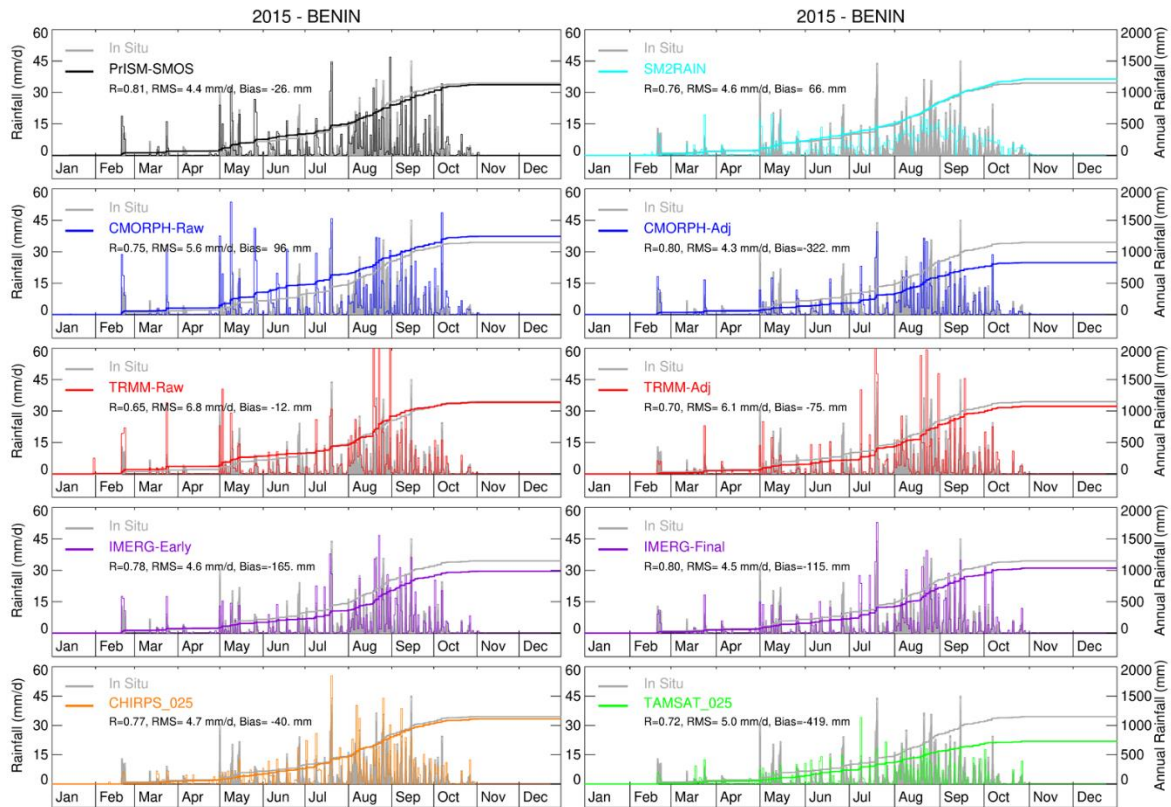
365 To enable fair comparison between satellite precipitation products, all products listed in Table 2
 366 were regridded to the 0.25° resolution and daily time-scale. At this spatial scale, a direct comparison
 367 with a single raingauge station can be distrusted due to the large spatial scale difference. Thus, we
 368 conducted a two-step assessment methodology. First, an accurate assessment was performed on two
 369 sites where 10 to 12 raingauge stations are located within the same pixel of 0.25° (i.e. about 25×25
 370 km^2) belonging to the AMMA-CATCH Observatory in Niger and Benin. As stated in section 2.1, the
 371 use of dense networks of rain gauges allows an accurate estimate of the precipitation rate at this scale.

372 In a second step, a direct, less relevant comparison between satellite (0.25°) and individual rainfall
373 station was done and results were analyzed at the network scale, i.e. Burkina Faso (20 stations),
374 Central Africa (42 stations) and East Africa (78 stations).

375 3.1. Assessment at the local scale (Niger and Benin)

376 The eleven selected precipitation products were compared to ground-based precipitation
377 measurements using commonly used statistical scores: the Pearson correlation (R), the Root Mean
378 Square Error (RMSE in mm/day) and the annual bias (in mm). Null values were accounted for in the
379 scores calculation and the comparison was performed at the daily time scale and at the 0.25° spatial
380 resolution. As the ground-based precipitation datasets (Niger and Benin) are available at the hourly
381 time scale whereas some satellite products are provided at the daily time scale, the matching of the
382 two time-series was carefully checked to avoid the known ambiguity between a 6am-6am day
383 (commonly used in precipitation measurements) and a 0-24h day. Lastly, we also examine the
384 number of rainy days (cumulative daily rainfall > 1 mm) compared to in situ measurements.
385

386 Results are presented for illustrative purposes for the Benin site (2015) in Figure 3. Statistical
387 scores (R, RMSE and annual bias) are plotted in each graph and are also reported in Table 3. Overall,
388 all products capture relatively well the temporal dynamics of precipitation with a rather high
389 correlation coefficient ($R > 0.70$ except for TRMM-Raw ($R = 0.65$) and GPCC ($R = 0.42$) reported only in
390 Table 3). Best performances in term of correlation are obtained by PrISM ($R = 0.81$), CMORPH-Adj,
391 IMERG-Final ($R = 0.80$), IMERG-Early ($R = 0.78$) and CHIRPS ($R = 0.77$). Regarding RMSE, best
392 performances are obtained by CMORPH-Adj, PrISM, IMERG-Final and SM2RAIN and IMERG-Early
393 with RMSE values equal to 4.3, 4.4, 4.5 and 4.6 mm/day respectively. Lowest performances are
394 obtained by TRMM-Raw and GPCC with 6.8 mm/day. Regarding bias score, four products obtained
395 annual cumulative precipitation values very close to the observation (1150 mm): TRMM-Raw (1138
396 mm, -1%), PrISM (1124 mm, -2.3%), CHIRPS (1110 mm, -4.3%) and SM2RAIN (1216 mm, +5.7%). On
397 the contrary, TAMSAT_025 strongly underestimates the annual precipitation with an estimation of
398 only 731 mm (-36%). Surprisingly, the three adjusted products (CMORPH-Adj, TRMM-Adj and
399 IMERG-Final) provide moderate to strong underestimated precipitation (respectively 828 mm (-28%),
400 1075 mm (-6.5%) and 1035 mm (-10%) compared to in situ precipitation measurements. Similarly,
401 GPCC exhibits moderate underestimation (1013 mm, -12%). Only the CMORPH-Raw product shows
402 an overestimation of the annual rainfall with 1246 mm (+8%) in Benin in 2015. Lastly, Table 3 includes
403 the difference in term of annual rainy days. In the Benin site, 103 rainy days (> 1mm) were observed
404 in 2015. Table 3 shows that CHIRPS, GPCC and SM2RAIN tends to overestimate this number (112,
405 135 and 168 days respectively) whereas PrISM and CMORPH-Raw provides similar number of rainy
406 days (101 and 102 days respectively). All other precipitation products exhibit a slight underestimation
407 (from 88 to 94 days).
408



409
 410 **Figure 3 :** Example of comparison between in situ precipitation measurements (Benin 0.25° site, 2015, in grey)
 411 and the ten precipitation products (PrISM, SM2RAIN, CMORPH (Raw and Adj), TRMM (Raw and Adj), IMERG
 412 (Early and Final), CHIRPS-025 and TAMSAT-025). Bars show daily rainfall amounts (left axis), curves show
 413 cumulative rainfall (right axis). Statistical scores are reported in Table 3.
 414

415 The same analysis was conducted for the Niger site in 2015. Graphics are shown in
 416 supplementary materiel (Figure S1) and the statistical scores are reported in Table 3. Similarly, the
 417 CMORPH-Adj and PrISM products obtain good performances in term of correlation ($R=0.82$ and
 418 $R=0.81$ respectively) and GPCP obtains the lower score ($R=0.33$) probably due to the low density of
 419 gauges in the Niger region and its original spatial resolution of 1° . Regarding the RMSE scores, best
 420 performances are obtained by PrISM, TAMSAT-025, CHIRPS, TRMM-Adj, SM2RAIN, CMORPH-Adj
 421 and IMERG-Final (from 3.7 mm/day to 4.6 mm/day). Conversely, CMORPH-Raw and TRMM-Raw
 422 products obtain lower RMSE scores (6.7 and 6.9 mm/day). In term of annual bias, four products
 423 obtained annual cumulative precipitation values quite close to the observation (601 mm): TRMM-Adj
 424 (602 mm), IMERG-Final (547 mm, -9%), PrISM (669 mm, +11%) and IMERG-Early (687 mm, +14%).
 425 On the contrary, CMORPH-Raw and TRMM-Raw strongly overestimate annual precipitation (1052
 426 mm, +75% and 1090 mm, +81% respectively). Other products obtain intermediate annual bias (see
 427 Table 3). Regarding the number of rainy days in Niger (43 days from in situ measurements), best
 428 performances were obtained by SM2RAIN, TAMSAT_025 and CMORPH-Adj (48, 50 and 51 days
 429 respectively) whereas GPCP still provides an overestimated number of rainy days (71 days). Other
 430 products, PrISM included, provide a slight overestimation of the number of rainy days compared to
 431 observations (from 52 to 57 days).

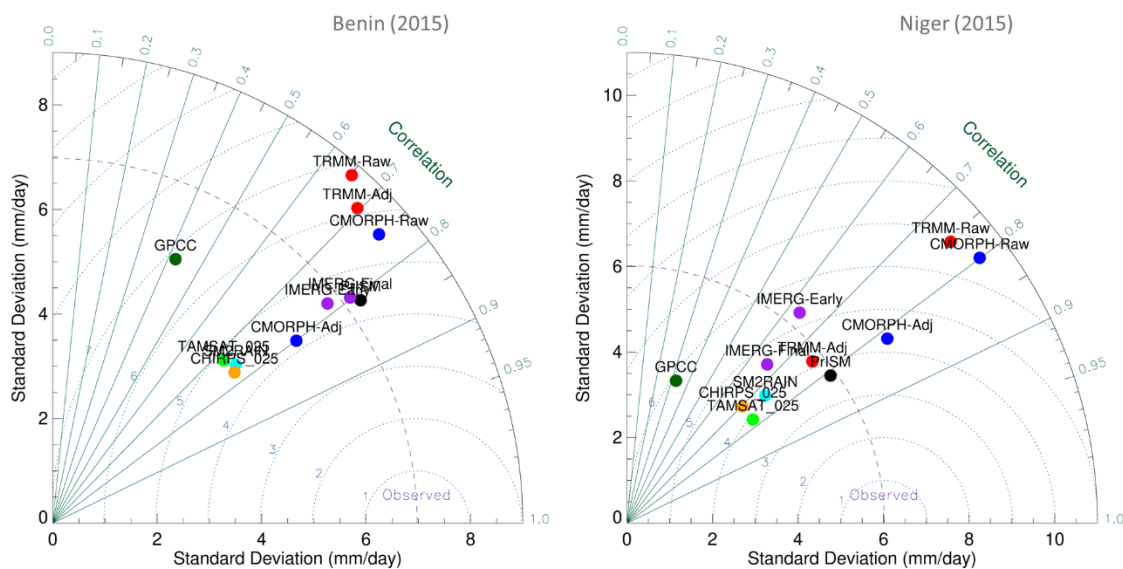
432
 433 **Table 3.** Statistical scores (R, RMSE, annual bias and nb of rainy days) between in situ precipitations
 434 measurements (Benin and Niger, 2015) and the eleven precipitation products. Bold values indicate the best
 435 performances. There are 103 rainy days in Benin and 43 rainy days in Niger in 2015.

2015	Benin 0.25° (1150 mm, 103 rainy days)	Niger 0.25° (601 mm, 43 rainy days)
------	---------------------------------------	-------------------------------------

	R	RMSE (mm/d)	Bias (mm)	Rainy days (>1mm/d)	R	RMSE (mm/d)	Bias (mm)	Rainy days (>1mm/d)
PrISM	0.81	4.4	-26	101	0.81	3.7	+68	55
CMORPH-Raw	0.75	5.6	+96	102	0.80	6.7	+451	56
TRMM-Raw	0.65	6.8	-12	94	0.75	6.9	+489	54
IMERG-Early	0.78	4.6	-165	90	0.63	5.3	+86	57
TAMSAT-025	0.72	5.0	-419	92	0.77	3.9	-169	50
SM2RAIN	0.76	4.6	+66	168	0.74	4.1	-203	48
CHIRPS	0.77	4.7	-40	112	0.70	4.3	-138	55
GPCC	0.42	6.8	-137	135	0.33	5.9	-147	71
CMORPH-Adj	0.80	4.3	-322	88	0.82	4.3	+152	51
TRMM-Adj	0.70	6.1	-75	92	0.75	4.1	+1	53
IMERG-Final	0.80	4.5	-115	94	0.66	4.6	-54	52

436
437
438
439
440
441
442
443
444
445
446
447
448

Figure 4 shows the Taylor diagrams [57] in Benin and Niger sites daily precipitation in 2015. Taylor diagram enables a visual comparative assessment of the different precipitation products quantifying the degree of correspondence between the estimated and observed precipitation in terms of three statistics: the Pearson correlation coefficient, the root-mean-square error (RMSE), and the standard deviation. Correlation scores are plotted as the radial lines, and the linear distance of a point to the Observed point indicates the RMSE from in situ measurements. For instance, the GPCC point for Benin site is close to the 0.4 radial line (R=0.42 in Table 3) and close to the “7” dotted circle (RMSE=6.8 mm/days). Graphically, the best products are those closest to the “Observed” point and to the dashed curve which indicates the same amplitude of the variations. In Benin (2015), those best products are the two IMERG products and the PrISM product. For Niger (2015), PrISM and TRMM-Adj perform better than the other ones.

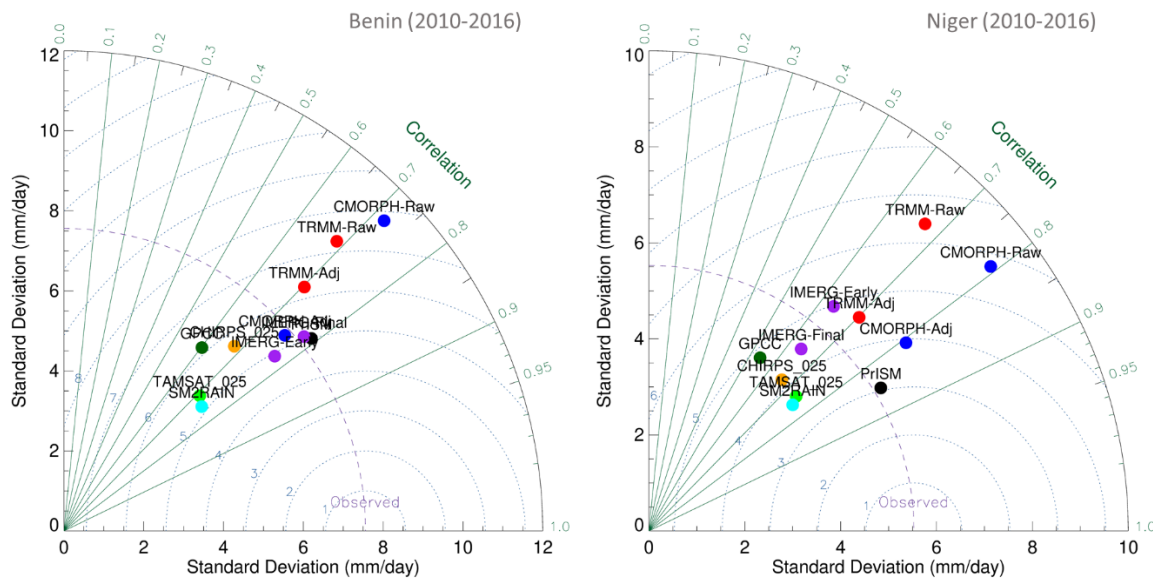


449
450
451
452
453
454
455

Figure 4: Taylor diagrams for the Benin (left) and Niger (right) 0.25° sites for the year 2015 for the 11 precipitation products. Color dots refer to the different products (blue=CMORPH, red=TRMM, purple=IMERG, green=TAMSAT_025, cyan=SM2RAIN, orange=CHIRPS, dark green=GPCC and black=PrISM). Statistical scores are given in Table 3.

Lastly, the Taylor diagrams were plotted for the whole period (2010-2016, instead of 2015) except for the two IMERG and SM2RAIN precipitation products that start in March 2014 and are then

456 considered only for 2015-2016 period. Figure 5 reveals some slight differences compared to Figure 4
 457 but leads to similar conclusions. Globally, when a product is provided in two versions, e.g. raw and
 458 adjusted, the adjusted product performs better. The “raw” version of TRMM and CMORPH are
 459 located far away from their adjusted versions. The PrISM product was found to be among the best
 460 products for the Benin site and provides the best performance for the Niger site. TAMSAT_025 and
 461 SM2RAIN have similar scores and perform better for the Niger site but their standard-deviations are
 462 much lower than in the observation.
 463
 464



465
 466 **Figure 5:** Taylor diagrams for the Benin (left) and Niger (right) 0.25° sites and the 2010-2016 period (except for
 467 IMERG, 2015-2016) and the 11 precipitation products. Color dots refer to the different products (blue=CMORPH,
 468 red=TRMM, purple=IMERG, green=TAMSAT_025, cyan=SM2RAIN, orange=GPCC and black=PrISM).

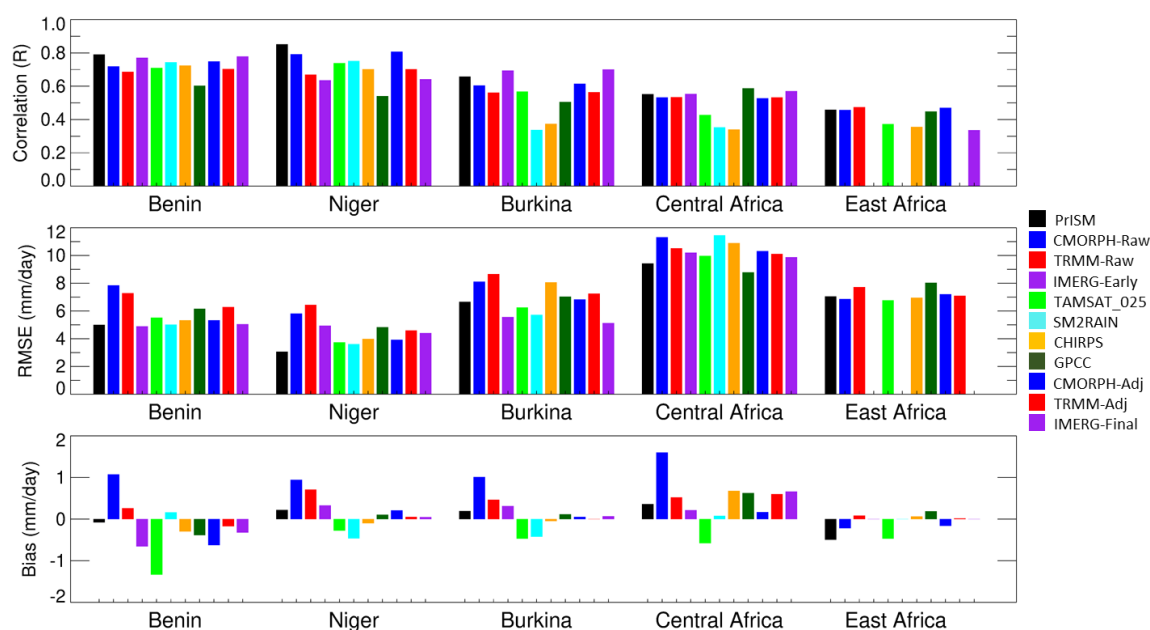
469

470 3.2. Assessment at the regional scale

471 At the regional scale, scores were calculated using individual raingauge stations compared to
 472 0.25° precipitation products. Scores were calculated at the daily time scale based on the whole
 473 available period (see Table 1). Then, the median value of all individual scores (R, RMSE and bias) was
 474 calculated. Results are presented separately for the three raingauge networks (Burkina Faso, Central
 475 Africa and East Africa) in Figure 6. Results obtained for Benin and Niger are also reported in Figure
 476 6 for comparison. Note that the two IMERG products were not considered for East Africa because the
 477 ground rainfall measurements were not available after 2013.
 478

479 Results show globally that the correlation score is slightly lower for Burkina, Central Africa and
 480 East Africa compared to Benin and Niger. Similarly, the corresponding RMSE are respectively greater
 481 (worse) for these three networks. On the other hand, the biases are in the same order of magnitude
 482 in the five regions. In all regions, PrISM shows good performances according to the 3 scores and is
 483 among the best products together with the two IMERG products. It can be observed that PrISM
 484 systematically outperforms CMORPH-Raw in term of RMSE (except in East Africa where it is slightly
 485 less performant). But the improvement in term of correlation is more modest. CMORPH and TRMM,
 486 in their adjusted or raw versions, show similar performances in terms of correlation but provide
 487 generally much better results in term of RMSE and biases for their adjusted versions. SM2RAIN and
 488 CHIRPS products show lower correlation and higher RMSE scores for Burkina-Faso and Central
 489 Africa but presents a low bias for all regions. Although its biases are small, GPCC, as expected from

490 its low original resolution, generally shows relatively low performances, except in Central Africa.
 491 Finally, TAMSAT_025 globally tends to underestimate the rainfall rate but shows relatively good
 492 correlation and RMSE scores.
 493



494 **Figure 6:** Statistical scores (R, RMSE and bias) for the five regions (Benin, Niger, Burkina-Faso, Central Africa
 495 and East Africa) and for the 11 precipitation products. The temporal period depends on the satellite product and
 496 in situ availabilities.
 497

498 4. Limitation of the PrISM methodology

499 One limitation of the methodology is that it is not able to create a rain event. This is clearly shown
 500 in Table 3 where the number of rainy days (> 1 mm) does not change much between the CMORPH-
 501 Raw product and the PrISM product. Therefore, it is necessary to use an initial precipitation product
 502 that overestimates the number of events since the PrISM algorithm is able to reduce the amount of
 503 rainfall.
 504

505 The PrISM algorithm was also found to be more efficient when the initial rainfall product
 506 overestimates the annual rainfall amount. This is particularly true in East Africa where the CMORPH-
 507 Raw showed a negative annual bias (see Figure 6) and the PrISM algorithm was not able to correct
 508 for that underestimation. On the contrary, on the other 4 sites, the CMORPH-Raw showed positive
 509 annual biases which are suitably corrected by PrISM. The reason for this behavior is that a 10 mm
 510 rain event (for instance) can easily be reduced to 1 mm, but the PrISM algorithm can't propose a
 511 correction greater than 20 mm (correction factor ranging between 0 and 2). Consequently, it is easier
 512 to reduce the rainfall amount than to increase it.
 513

514 The satisfactory results of the PrISM methodology in Central Africa are a pleasant surprise since
 515 the SMOS soil moisture retrievals under dense forest are expected to be inaccurate. The explanation
 516 of this results is partly due to the large overestimation of the CMORPH-Raw product in Central
 517 Africa. The PrISM methodology leads to reduce the rainfall amount of most events and, mechanically,
 518 RMSE is reduced as well as the annual bias. Overall, the effect of vegetation cover on the performance
 519 of the PrISM algorithm is difficult to evaluate. Indeed, areas of dense vegetation are at the same time
 520 areas where the SMOS signal can be inaccurate but also areas of heavy precipitation with a high
 521 potential for improvement. PrISM performances are similar in Niger (low vegetation) and in Benin
 522

523 (medium vegetation), and the PrISM performances in Central Africa are better than in East Africa (in
524 term of correlation and bias correction).

525 4. Summary and next step

526

527 This study presents the PrISM algorithm and its evaluation over 5 regions in Africa. PrISM
528 algorithm uses knowledge of soil water content (provided by SMOS soil moisture measurements) to
529 adjust the precipitation rate of an existing satellite product (CMORPH-raw in this study). To assess
530 the benefit of the proposed methodology, PrISM was compared against ten state-of-the-art satellite
531 and ground-based rainfall products for five rain gauge networks located in semi-arid to wet areas in
532 Africa.

533

534 PrISM was found to generally outperform all real-time products (CMORPH-Raw, TRMM-Raw,
535 IMERG-Early, TAMSAT_025 and SM2RAIN), especially when considering areas where there exists a
536 dense network of rain gauge stations as a reference data set. It showed same or even better
537 performances than adjusted or post-processed products. The main contribution of PrISM is that it
538 greatly decreases RMSE values and reduces the bias values compared with the original CMORPH-
539 Raw product. Results in term of correlations are more modest. This result is quite important for many
540 applications that require real-time information on precipitation such as crop yield estimates, flood
541 nowcasting, dam management, ground-water recharge estimates and irrigation demand over large
542 areas.

543

544 Future studies will be designed to apply PrISM algorithm to other satellite soil moisture dataset
545 such as SMAP, ASCAT or SMOS-IC. At the moment, PrISM product is available on the ftp site:
546 ftp://ftp.ifremer.fr/Land_products/L4_PrISM/Africa/ and can be downloaded at
547 <https://doi.org/10.5281/zenodo.3565610> at an annual latency. The near-real-time version of the
548 product will shortly be available on the external ERDDAP of IGE in Grenoble: [http://osug-smos-
549 rea.osug.fr:8081/erddap/index.html](http://osug-smos-rea.osug.fr:8081/erddap/index.html).

550 **Supplementary Materials:** The following are available online at www.mdpi.com/xxx/s1, Figure S1: Comparison
551 between in situ precipitation measurements (Niger 0.25° site, 2015, in grey) and the ten precipitation products
552 (PrISM, CMORPH (Raw and Adj), TRMM (Raw and Adj), IMERG (Early and Final), TAMSAT-025, CHIRPS and
553 SM2RAIN). Statistical scores are reported in Table 3.

554 **Author Contributions:** T. P. proposed the idea, carried out the experimental design, analyzed the data, and
555 wrote the paper. C. R.-C. and B. P. participated to the PrIMS algorithm development and validation, C. B, P. C.,
556 N. P. and G.P. provide in situ rainfall data; G. Q. help in the visualization, L. B. and C. M. provide SM2RAIN
557 product and contribute to the writing of the paper. Y. K. contribute to the original idea and to the writing of the
558 paper.

559 **Funding:** This research was funded by ESA, grant number ESA/AO/1-7875/14/I-NC (4000114738/15/I-SBO). This
560 research also benefits from TOSCA (CNES, Centre national d'études spatiales, France).

561 **Acknowledgments:** The authors would like to thank University of Douala, University of Bangui, University
562 Omar-Bongo in Libreville, University of Liège, CIRAD Montpellier for providing precipitation data in Central
563 Africa, and National Meteorological Department of Burkina Faso.

564

565 References

566

- 567 1. Sultan, B.; Barbier, B.; Fortilus, J.; Mbaye, S.M.; Leclerc, G. Estimating the Potential Economic Value of
568 Seasonal Forecasts in West Africa: A Long-Term Ex-Ante Assessment in Senegal. *Weather Climate and
569 Society* **2010**, *2*, 69-87, doi:10.1175/2009wcas1022.1.

- 570 2. Washington, R.; Harrison, M.; Conway, D.; Black, E.; Challinor, A.; Grimes, D.; Jones, R.; Morse, A.; Kay,
571 G.; Todd, M. African climate change - Taking the shorter route. *Bulletin of the American Meteorological Society*
572 **2006**, *87*, 1355+, doi:10.1175/bams-87-10-1355.
- 573 3. Nicholson, S.E.; Some, B.; McCollum, J.; Nelkin, E.; Klotter, D.; Berte, Y.; Diallo, B.M.; Gaye, I.; Kpabeba, G.;
574 Ndiaye, O., et al. Validation of TRMM and other rainfall estimates with a high-density gauge dataset for
575 West Africa. Part I: Validation of GPCC rainfall product and pre-TRMM satellite and blended products.
576 *Journal of Applied Meteorology* **2003**, *42*, 1337-1354, doi:10.1175/1520-0450(2003)042<1337:votaor>2.0.co;2.
- 577 4. Gosset, M.; Viarre, J.; Quantin, G.; Alcoba, M. Evaluation of several rainfall products used for hydrological
578 applications over West Africa using two high-resolution gauge networks. *Quarterly Journal of the Royal*
579 *Meteorological Society* **2013**, *139*, 923-940, doi:10.1002/qj.2130
- 580 5. Camberlin, P.; Barraud, G.; Bigot, S.; Dewitte, O.; Imwangana, F.M.; Mateso, J.C.M.; Martiny, N.;
581 Monsieurs, E.; Moron, V.; Pellarin, T., et al. Evaluation of remotely sensed rainfall products over Central
582 Africa. *Quarterly Journal of the Royal Meteorological Society* **2019**, *145*, 2115-2138, doi:10.1002/qj.3547.
- 583 6. Serrat-Capdevila, A.; Merino, M.; Valdes, J.B.; Durcik, M. Evaluation of the Performance of Three Satellite
584 Precipitation Products over Africa. *Remote Sensing* **2016**, *8*, doi:10.3390/rs8100836.
- 585 7. Pomeon, T.; Jackisch, D.; Diekkruger, B. Evaluating the performance of remotely sensed and reanalysed
586 precipitation data over West Africa using HBV light. *Journal of Hydrology* **2017**, *547*, 222-235,
587 doi:10.1016/j.jhydrol.2017.01.055.
- 588 8. Maidment, R.I.; Grimes, D.I.F.; Allan, R.P.; Greatrex, H.; Rojas, O.; Leo, O. Evaluation of satellite-based and
589 model re-analysis rainfall estimates for Uganda. *Meteorological Applications* **2013**, *20*, 308-317,
590 doi:10.1002/met.1283.
- 591 9. Roca, R.; Chambon, P.; Jobard, I.; Kirstetter, P.E. Comparing Satellite and Surface Rainfall Products over
592 West Africa at Meteorologically Relevant Scales during the AMMA Campaign Using Error Estimates.
593 *Journal of Applied Meteorology and Climatology* **2010**, *49*, 715-731, doi:10.1175/2009jamec2318.1.
- 594 10. Jobard, I.; Chopin, F.; Berges, J.C.; Roca, R. An intercomparison of 10-day satellite precipitation products
595 during West African monsoon. *International Journal of Remote Sensing* **2011**, *32*, 2353-2376,
596 doi:10.1080/01431161003698286.
- 597 11. Maggioni, V.; Sapiano, M.R.P.; Adler, R.F. Estimating Uncertainties in High-Resolution Satellite
598 Precipitation Products: Systematic or Random Error? *Journal of Hydrometeorology* **2016**, *17*, 1119-1129,
599 doi:10.1175/jhm-d-15-0094.1.
- 600 12. Pan, M.; Wood, E.F.; Wojcik, R.; McCabe, M.F. Estimation of regional terrestrial water cycle using multi-
601 sensor remote sensing observations and data assimilation. *Remote Sensing of Environment* **2008**, *112*, 1282-
602 1294, doi:10.1016/j.rse.2007.02.039.
- 603 13. Crow, W.T. A novel method for quantifying value in spaceborne soil moisture retrievals. *Journal of*
604 *Hydrometeorology* **2007**, *8*, 56-67.
- 605 14. Pellarin, T.; Ali, A.; Chopin, F.; Jobard, I.; Berges, J.C. Using spaceborne surface soil moisture to constrain
606 satellite precipitation estimates over West Africa. *Geophysical Research Letters* **2008**, *35*
- 607 15. McCabe, M.F.; Wood, E.F.; Wojcik, R.; Pan, M.; Sheffield, J.; Gao, H.; Su, H. Hydrological consistency using
608 multi-sensor remote sensing data for water and energy cycle studies. *Remote Sensing of Environment* **2008**,
609 *112*, 430-444, doi:10.1016/j.rse.2007.03.027.
- 610 16. Crow, W.T.; Huffman, G.J.; Bindlish, R.; Jackson, T.J. Improving Satellite-Based Rainfall Accumulation
611 Estimates Using Spaceborne Surface Soil Moisture Retrievals. *Journal of Hydrometeorology* **2009**, *10*, 199-212,
612 doi:10.1175/2008jhm986.1.
- 613 17. Pellarin, T.; Tran, T.; Cohard, J.M.; Galle, S.; Laurent, J.P.; de Rosnay, P.; Vischel, T. Soil moisture mapping
614 over West Africa with a 30-min temporal resolution using AMSR-E observations and a satellite-based
615 rainfall product. *Hydrology and Earth System Sciences* **2009**, *13*, 1887-1896.
- 616 18. Brocca, L.; Moramarco, T.; Melone, F.; Wagner, W. A new method for rainfall estimation through soil
617 moisture observations. *Geophysical Research Letters* **2013**, *40*, 853-858, doi:10.1002/grl.50173.
- 618 19. Brocca, L.; Ciabatta, L.; Massari, C.; Moramarco, T.; Hahn, S.; Hasenauer, S.; Kidd, R.; Dorigo, W.; Wagner,
619 W.; Levizzani, V. Soil as a natural rain gauge: Estimating global rainfall from satellite soil moisture data.
620 *Journal of Geophysical Research-Atmospheres* **2014**, *119*, 5128-5141, doi:10.1002/2014jd021489.
- 621 20. Koster, R.D.; Brocca, L.; Crow, W.T.; Burgin, M.S.; De Lannoy, G.J.M. Precipitation estimation using L-band
622 and C-band soil moisture retrievals. *Water Resources Research* **2016**, *52*, 7213-7225,
623 doi:10.1002/2016wr019024.

- 624 21. Massari, C.; Crow, W.; Brocca, L. An assessment of the performance of global rainfall estimates without
625 ground-based observations. *Hydrology and Earth System Sciences* **2017**, *21*, 4347-4361, doi:10.5194/hess-21-
626 4347-2017.
- 627 22. Wanders, N.; Pan, M.; Wood, E.F. Correction of real-time satellite precipitation with multi-sensor satellite
628 observations of land surface variables. *Remote Sensing of Environment* **2015**, *160*, 206-221,
629 doi:10.1016/j.rse.2015.01.016.
- 630 23. Brocca, L.; Pellarin, T.; Crow, W.T.; Ciabatta, L.; Massari, C.; Ryu, D.; Su, C.H.; Rudiger, C.; Kerr, Y. Rainfall
631 estimation by inverting SMOS soil moisture estimates: A comparison of different methods over Australia.
632 *Journal of Geophysical Research-Atmospheres* **2016**, *121*, 12062-12079, doi:10.1002/2016jd025382.
- 633 24. Román-Cascón, C.; Pellarin, T.; Gibon, F.; Brocca, L.; Cosme, E.; Crow, W.; Fernandez-Prieto, D.; Kerr, Y.H.;
634 Massari, C. Correcting satellite-based precipitation products through SMOS soil moisture data assimilation
635 in two land-surface models of different complexity: API and SURFEX. *Remote Sensing of Environment* **2017**,
636 *200*, 295-310, doi:10.1016/j.rse.2017.08.022.
- 637 25. Zhang, Z.; Wang, D.G.; Wang, G.L.; Qiu, J.X.; Liao, W.L. Use of SMAP Soil Moisture and Fitting Methods
638 in Improving GPM Estimation in Near Real Time. *Remote Sensing* **2019**, *11*, doi:10.3390/rs11030368.
- 639 26. Schamm, K.; Ziese, M.; Becker, A.; Finger, P.; Meyer-Christoffer, A.; Schneider, U.; Schroder, M.; Stender,
640 P. Global gridded precipitation over land: a description of the new GPCP First Guess Daily product. *Earth
641 System Science Data* **2014**, *6*, 49-60, doi:10.5194/essd-6-49-2014.
- 642 27. Adler, R.F.; Huffman, G.J.; Chang, A.; Ferraro, R.; Xie, P.P.; Janowiak, J.; Rudolf, B.; Schneider, U.; Curtis,
643 S.; Bolvin, D., et al. The version-2 global precipitation climatology project (GPCP) monthly precipitation
644 analysis (1979-present). *Journal of Hydrometeorology* **2003**, *4*, 1147-1167.
- 645 28. Adler, R.F.; Sapiiano, M.R.P.; Huffman, G.J.; Wang, J.J.; Gu, G.J.; Bolvin, D.; Chiu, L.; Schneider, U.; Becker,
646 A.; Nelkin, E., et al. The Global Precipitation Climatology Project (GPCP) Monthly Analysis (New Version
647 2.3) and a Review of 2017 Global Precipitation. *Atmosphere* **2018**, *9*, doi:10.3390/atmos9040138.
- 648 29. New, M.; Lister, D.; Hulme, M.; Makin, I. A high-resolution data set of surface climate over global land
649 areas. *Climate Research* **2002**, *21*, 1-25, doi:10.3354/cr021001.
- 650 30. Galle, S.; Grippa, M.; Peugeot, C.; Moussa, I.B.; Cappelaere, B.; Demarty, J.; Mougou, E.; Panthou, G.;
651 Adjomayi, P.; Agbossou, E.K., et al. AMMA-CATCH, a Critical Zone Observatory in West Africa
652 Monitoring a Region in Transition. *Vadose Zone Journal* **2018**, *17*, doi:10.2136/vzj2018.03.0062.
- 653 31. Lebel, T.; Cappelaere, B.; Galle, S.; Hanan, N.; Kergoat, L.; Levis, S.; Vieux, B.; Descroix, L.; Gosset, M.;
654 Mougou, E., et al. AMMA-CATCH studies in the Sahelian region of West-Africa: An overview. *Journal of
655 Hydrology* **2009**, *375*, 3-13, doi:10.1016/j.jhydrol.2009.03.020.
- 656 32. Camberlin, P. 2017 : Temperature trends and variability in the Greater Horn of Africa: interactions with
657 precipitation. *Climate Dynamics*, *48*(1-2), 477-498. <https://doi.org/10.1007/s00382-016-3088-5>
- 658 33. Joyce, R.J.; Janowiak, J.E.; Arkin, P.A.; Xie, P.P. CMORPH: A method that produces global precipitation
659 estimates from passive microwave and infrared data at high spatial and temporal resolution. *Journal of
660 Hydrometeorology* **2004**, *5*, 487-503, doi:10.1175/1525-7541(2004)005<0487:camtpg>2.0.co;2.
- 661 34. Huffman, G.J.; Adler, R.F.; Bolvin, D.T.; Gu, G.J.; Nelkin, E.J.; Bowman, K.P.; Hong, Y.; Stocker, E.F.; Wolff,
662 D.B. The TRMM multisatellite precipitation analysis (TMPA): Quasi-global, multiyear, combined-sensor
663 precipitation estimates at fine scales. *Journal of Hydrometeorology* **2007**, *8*, 38-55, doi:10.1175/jhm560.1.
- 664 35. Huffman, G. J., D. T. Bolvin, and E. J. Nelkin, 2015: Day 1 IMERG final run release notes. NASA Doc., 9 pp.,
665 https://pmm.nasa.gov/sites/default/files/document_files/IMERG_FinalRun_Day1_release_notes.pdf.
- 666 36. Massari C., L. Brocca, T. Pellarin, G. Abramowitz, P. Filippucci, L. Ciabatta, V. Maggioni, Y. Kerr, and D.
667 Fernandez Prieto. A daily/25km short-latency rainfall product for data scarce regions based on the
668 integration of the GPM IMERG Early Run with multiple satellite soil moisture products. *Hydrology and
669 Earth System Sciences Disc.* **2019**, doi.org/10.5194/hess-2019-387
- 670 37. Thorne, V.; Coakley, P.; Grimes, D.; Dugdale, G. Comparison of TAMSAT and CPC rainfall estimates with
671 raingauges, for southern Africa. *International Journal of Remote Sensing* **2001**, *22*, 1951-1974,
672 doi:10.1080/01431160118816.
- 673 38. Maidment, R.I.; Grimes, D.; Black, E.; Tarnavsky, E.; Young, M.; Greatrex, H.; Allan, R.P.; Stein, T.; Nkonde,
674 E.; Senkunda, S., et al. Data Descriptor: A new, long-term daily satellite-based rainfall dataset for
675 operational monitoring in Africa. *Scientific Data* **2017**, *4*, doi:10.1038/sdata.2017.63.

- 676 39. Tarnavsky, E.; Grimes, D.; Maidment, R.; Black, E.; Allan, R.P.; Stringer, M.; Chadwick, R.; Kayitakire, F.
677 Extension of the TAMSAT Satellite-Based Rainfall Monitoring over Africa and from 1983 to Present. *Journal*
678 *of Applied Meteorology and Climatology* **2014**, *53*, 2805-2822, doi:10.1175/jamc-d-14-0016.1.
- 679 40. Maidment, R.I.; Grimes, D.; Allan, R.P.; Tarnavsky, E.; Stringer, M.; Hewison, T.; Roebeling, R.; Black, E.
680 The 30 year TAMSAT African Rainfall Climatology And Time series (TARCAT) data set. *Journal of*
681 *Geophysical Research-Atmospheres* **2014**, *119*, 10619-10644, doi:10.1002/2014jd021927.
- 682 41. Funk, C.; Peterson, P.; Landsfeld, M.; Pedreros, D.; Verdin, J.; Shukla, S.; Husak, G.; Rowland, J.; Harrison,
683 L.; Hoell, A., et al. The climate hazards infrared precipitation with stations-a new environmental record for
684 monitoring extremes. *Scientific Data* **2015**, *2*, doi:10.1038/sdata.2015.66.
- 685 42. Brocca, L.; Massari, C.; Ciabatta, L.; Moramarco, T.; Penna, D.; Zuecco, G.; Pianezzola, L.; Borga, M.;
686 Matgen, P.; Martinez-Fernandez, J. Rainfall estimation from in situ soil moisture observations at several
687 sites in Europe: an evaluation of the SM2RAIN algorithm. *Journal of Hydrology and Hydromechanics* **2015**, *63*,
688 201-209, doi:10.1515/johh-2015-0016.
- 689 43. Ciabatta, L.; Marra, A.C.; Panegrossi, G.; Casella, D.; Sano, P.; Dietrich, S.; Massari, C.; Brocca, L. Daily
690 precipitation estimation through different microwave sensors: Verification study over Italy. *Journal of*
691 *Hydrology* **2017**, *545*, 436-450, doi:10.1016/j.jhydrol.2016.12.057.
- 692 44. Massari, C.; Brocca, L.; Moramarco, T.; Trambly, Y.; Lescot, J.-F.D. Potential of soil moisture observations
693 in flood modelling: Estimating initial conditions and correcting rainfall. *Advances in Water Resources* **2014**,
694 *74*, 44-53, doi:10.1016/j.advwatres.2014.08.004.
- 695 45. Product User Manual (PUM): Soil Moisture Data Records, Metop ASCAT Soil Moisture Time Series, Tech.
696 Rep. Doc. No: SAF/HSAF/CDOP3/PUM, version 0.7, 2018.
- 697 46. Bishop, C.H.; Abramowitz, G. Climate model dependence and the replicate Earth paradigm. *Climate*
698 *Dynamics* **2013**, *41*, 885-900, doi:10.1007/s00382-012-1610-y.
- 699 47. Hobeichi, S.; Abramowitz, G.; Evans, J.; Ukkola, A. Derived Optimal Linear Combination
700 Evapotranspiration (DOLCE): a global gridded synthesis ET estimate. *Hydrology and Earth System Sciences*
701 **2018**, *22*, 1317-1336, doi:10.5194/hess-22-1317-2018.
- 702 48. Kerr, Y.H.; Waldteufel, P.; Wigneron, J.P.; Martinuzzi, J.M.; Font, J.; Berger, M. Soil moisture retrieval from
703 space: The Soil Moisture and Ocean Salinity (SMOS) mission. *Ieee Transactions on Geoscience and Remote*
704 *Sensing* **2001**, *39*, 1729-1735.
- 705 49. Kerr, Y.H.; Al-Yaari, A.; Rodriguez-Fernandez, N.; Parrens, M.; Molero, B.; Leroux, D.; Bircher, S.;
706 Mahmoodi, A.; Mialon, A.; Richaume, P., et al. Overview of SMOS performance in terms of global soil
707 moisture monitoring after six years in operation. *Remote Sensing of Environment* **2016**, *180*, 40-63,
708 doi:10.1016/j.rse.2016.02.042.
- 709 50. Pellarin, T.; Louvet, S.; Gruhier, C.; Quantin, G.; Legout, C. A simple and effective method for correcting
710 soil moisture and precipitation estimates using AMSR-E measurements. *Remote Sensing of Environment*
711 **2013**, *136*, 28-36, doi:10.1016/j.rse.2013.04.011.
- 712 51. Doucet, A.; Godsill, S.; Andrieu, C. On sequential Monte Carlo sampling methods for Bayesian filtering.
713 *Statistics and Computing* **2000**, *10*, 197-208, doi:10.1023/a:1008935410038.
- 714 52. Moradkhani, H.; Hsu, K.L.; Gupta, H.; Sorooshian, S. Uncertainty assessment of hydrologic model states
715 and parameters: Sequential data assimilation using the particle filter. *Water Resources Research* **2005**, *41*,
716 doi:10.1029/2004wr003604.
- 717 53. van Leeuwen, P.J. Particle Filtering in Geophysical Systems. *Monthly Weather Review* **2009**, *137*, 4089-4114,
718 doi:10.1175/2009mwr2835.1.
- 719 54. Evensen, G. Sampling strategies and square root analysis schemes for the EnKF. *Ocean Dynamics* **2004**, *54*,
720 539-560, doi:10.1007/s10236-004-0099-2.
- 721 55. Reichle, R.H.; Crow, W.T.; Koster, R.D.; Sharif, H.O.; Mahanama, S.P.P. Contribution of soil moisture
722 retrievals to land data assimilation products. *Geophysical Research Letters* **2008**, *35*, doi:10.1029/2007gl031986.
- 723 56. Yan, H.X.; DeChant, C.M.; Moradkhani, H. Improving Soil Moisture Profile Prediction With the Particle
724 Filter-Markov Chain Monte Carlo Method. *Ieee Transactions on Geoscience and Remote Sensing* **2015**, *53*, 6134-
725 6147, doi:10.1109/tgrs.2015.2432067.
- 726 57. Taylor, K.E. Summarizing multiple aspects of model performance in a single diagram. *Journal of Geophysical*
727 *Research-Atmospheres* **2001**, *106*, 7183-7192, doi:10.1029/2000jd900719.
- 728 58.
- 729 59.

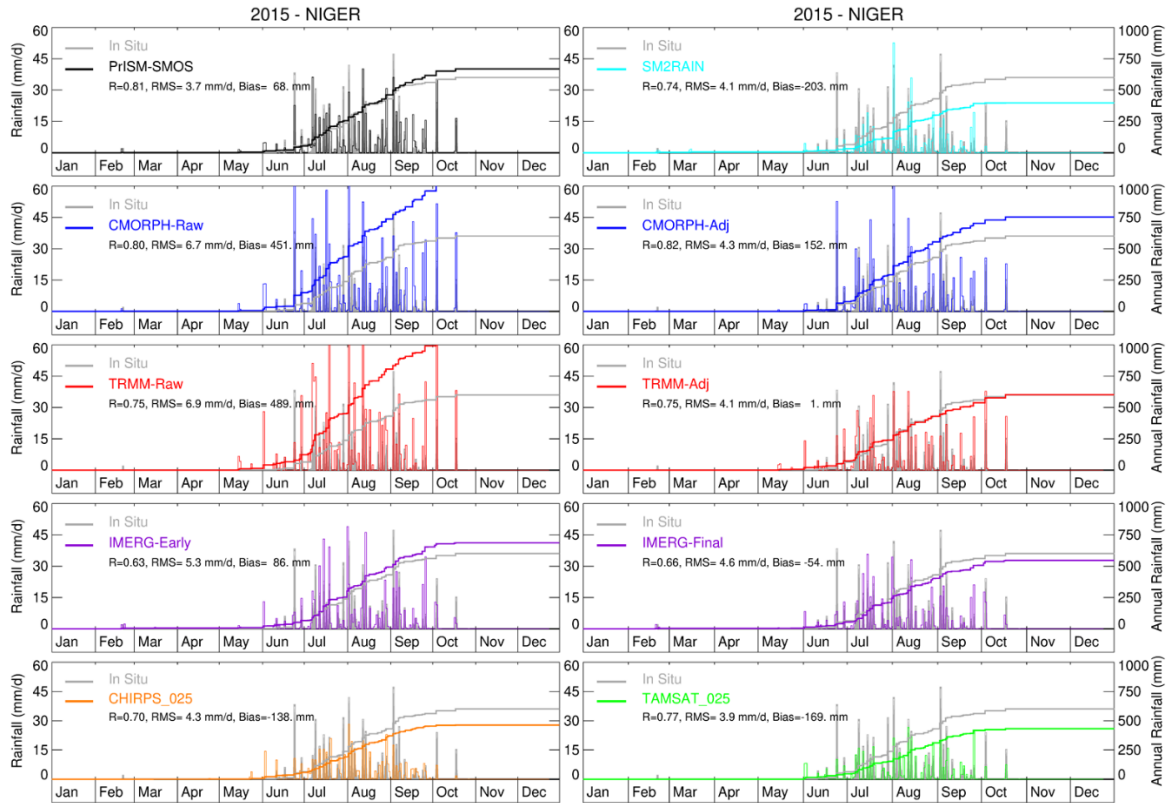
730



© 2019 by the authors. Submitted for possible open access publication under the terms and conditions of the Creative Commons Attribution (CC BY) license (<http://creativecommons.org/licenses/by/4.0/>).

731

732



733

734 **Figure S1:** Example of comparison between in situ precipitation measurements (Niger 0.25° site, 2015, in grey)
 735 and the ten precipitation products (PrISM, SM2RAIN, CMORPH (Raw and Adj), TRMM (Raw and Adj), IMERG
 736 (Early and Final), CHIRPS-025 and TAMSAT-025). Statistical scores are reported in **Table 3**.

737